Submitted: 09.06.2023.
Accepted for publication: 28.06.2023.

https://doi.org/10.2298/SOS230608036A

Characterization of NTC thick film thermistor paste $Cu_{0.2}Ni_{0.5}Zn_{1.0}Mn_{1.3}O_4$

Stanko O. Aleksić[1,*], Nina N. Obradović[2], Nebojša S. Mitrović[1], Miloljub D. Luković[3]

[1]Faculty of Technical Sciences, Čačak, Svetog Save 65, Čačak 32000, University of Kragujevac, Serbia

[2]Institute of Technical Sciences of SASA, Kneza Mihaila 35/IV, 1000 Belgrade, Serbia

[3]Information Technology School-ITS, Cara Dušana 34, Zemun 11080, Serbia

*Corresponding author: frakulah@gmail.com (Dr. Stanko Aleksić)

Abstract

A powder of $Cu_{0.2}Ni_{0.5}Zn_{1.0}$ $Mn_{1.3}O_4$ composition for custom thermistor was prepared by using the respective mixture of metal oxides and solid state reaction at 1000 °C/4h in air. The obtained thermistor powder was milled in the planetary ball mill and agate mill for a prolonged time to achieve submicron powder. The prepared thermistor powder was further characterized by using XRD and SEM techniques. After that, the thermistor powder was pressed into small disc-shaped samples and sintered at 1150 °C/2h. The sintered samples were also characterized by using XRD and SEM. The main electrical properties such as nominal resistance R and thermistor exponential factor B were measured in the climatic test chamber. After that, the thick film paste was prepared using the same powder, an organic vehicle and a glass frit. The paste was printed on alumina substrate, dried at 150 °C /30 min and sintered in air at 850 °C /10 min in a hybrid conveyor furnace. Planar electrodes were printed on the sintered NTC thermistor layer using PdAg thick film paste. The electric properties of the sintered thick film thermistor were also measured in the climatic test chamber. The obtained results were used for development of novel self-heating thermistor applications.

Keywords: NTC thick film thermistor; modified nickel manganite powder.

1. Introduction

PTC thermistors are a type of resistors the resistance of which exponentially increases with temperature, while NTC thermistors are a type of resistors the resistance of which exponentially decreases with higher temperature [1, 2]. They are widely used for temperature measurement, temperature control in household appliances and electronic equipment, temperature alarm switches, component for temperature compensation, time delay and other applications in automotive industry, telecommunications, meteorology, agriculture, healthcare, etc. [3, 4].

The PTC thermistors are usually made of barium titanates $BaTi0_3$ doped with Bi, Ta and other dopants [5, 6]. There is a group of metal oxide compounds commonly used for NTC thermistors in the temperature range from -30 to +120 °C such as $(NiMn)_3O_4$, $(NiMnCo)_3O_4$, $(NiMnFeCo)_3O_4$, $(Fe,Ti)_2O_3$, and others [7, 8]. The pure nickel manganite $NiMn_2O_4$ is suitable as kΩ resistance thermistor with moderate temperature exponential factor B [9, 10]. It is prepared by calcination of the powder mixture NiO and $MnCO_3$ at a ratio 1: 2 at 900-1000 °C/4h in air. It is possible to lower nominal resistance of nickel manganite by addition of other metal oxides to the initial metal oxide mixture, such as CuO, CoO, ZnO, ZrO_2, Y_2O_3, LiO, RuO_2, and others, [11-14].

The partial substitution of Mn and Ni with Cu and Zn changes the crystal structure of nickel manganite; e.g. it forms complex spinel and affects the thermistor semiconductor mechanism [15, 16]. The nickel manganite ($NiMn_2O_4$) has the structure of normal spinel $A^{2+}B_2^{3+}O_4$ (A=Ni, B=Mn). The tetrahedral ion Ni^{2+} and octahedral ion Mn^{3+} can exchange sites in the spinel [17,18]. In this way octahedral ions change the valence as $2Mn^{3+} \rightarrow (Mn^{2+}, Mn^{4+})$ e.g. ion Mn^{2+} fits the vacancy where ion Ni^{2+} is missing. This effect occurs in a very small amount but affects the semiconductor properties. The semiconductor properties of the thermistor such as electrical bulk resistivity, energy gap and exponential factor B can be modified in a certain range by this substitution mechanism to fulfil the customer requirements [19, 20].

In our experimental work a novel thermistor material based on modified nickel manganite $Cu_{0.2}Ni_{0.5}Zn_{1.0}Mn_{1.3}O_4$ was developed as custom designed thermistor material. Valence of Mn was the same in the initial and novel spinel, but introduction of Zn and Cu into the spinel causes a little smaller effective energy gap and lover NTC thermistor

exponential factor B. After that, a novel thick film thermistor paste was prepared using the same powder but additionally milled to achieve submicron particles. The objective was to develop a thick film self-heating thermistor with reduced dimensions and with optimized nominal resistance below 1kΩ. Such low nominal resistances were only suitable for the heat loss flowmeter application which was the final objective. The development of a novel thick film paste based on $Cu_{0.2}Ni_{0.5}Zn_{1.0}Mn_{1.3}O_4$ submicron powder was a necessary step in this investigation.

2. Materials and Experimental Procedures

The commercial metal oxide powders $MnCO_3$, NiO, CuO and ZnO (Sigma-Aldrich 99.5% purity, ~1 micron average powder particle size) were mixed in the stoichiometric molar ratio to form compound $Cu_{0.2}Ni_{0.5}Zn_{1.0}Mn_{1.3}O_4$. The metal oxide mixture was mechanically treated in the planetary ball mill (FRITSCH V) for 30 min (initial powder milling). After that, the mixture was calcinated at 1000 °C/4h to form thermistor grade material, while CO_2 was released during the solid state process. The calcinated material was milled thereafter in the planetary ball mill (FRITSCH V) for 2h and additionally in the agate mills for 48 h.

The obtained novel thermistor powder was analyzed by XRD (Philips PW1050). The novel powder was further analyzed using SEM (TESCAN-VEGA TS 5130MM). From the obtained powder small disc "green samples" (Φ=10 mm, h≈2.5mm) were pressed at 0.2 GPa. The pressed samples were sintered in air at different temperatures from 850 to 1250 °C /2h in steps of 50 °C in the chamber furnace. The bulk density was measured and after that, silver-epoxy paste was printed on both sides of the sintered discs to serve as electrodes for the subsequent electrical measurements. The bulk resistance vs. sintering temperature was also measured.

Thick film thermistor paste was prepared by using the obtained thermistor powder $Cu_{0.2}Ni_{0.5}Zn_{1.0}Mn_{1.3}O_4$, organic vehicle (ethyl cellulose) and borosilicate glass frits. The weight ratio was 70 g of thermistor powder, 30 g of organic vehicle and 5 g of glass frits of average particle size of 1.5 μm (ASAHI glass, Japan). The thermistor paste was screen

printed with screen SD 200 (stainless steel) on square thick film test geometry for resistors (Du Pont resistor test, 2.5mm x 2.5mm) with PdAg electrodes sintered at 850°C/10 min in conveyor furnace.

The thus obtained thermistor thick films of the novel grade were analyzed using SEM. The electrical characterization of the thick film was done in climatic test chamber: NTC curve was obtained and thermistor exponential factor B was determined. After that a thick film thermistor with reduced dimensions was printed and electrically characterized.

3. Results and Discussion

Using the procedure presented above modified spinel $Cu_{0.2}Ni_{0.5}Zn_{1.0}Mn_{1.3}O_4$ was obtained: the XR diffractogram is given in Figure 1. The characteristic plains in the complex spinel crystal lattice were recognized and marked on the diffractogram.

The achieved average powder particle size was in the range of 100 to 150 nm, while the size of agglomerates was in the range of 0.5 to 1.5 μm as given in Figure 2.

The SEM imaging revealed the presence of particle agglomeration produced during the milling process although previously being ultrasonically dispersed in ethyl alcohol.

The sintered samples were analyzed under SEM. The agglomerated particles re-crystallized to micron-sized grains as presented in Figure 3. The grains of pressed and sintered samples have average particle size around 1.45 μm and partly open porous structure.

The top view photography of the obtained disc samples with and without electrodes is given in Figure 4.

The bulk thermistor resistivity ρ is calculated from the disc thermistor nominal resistances R measured at room temperature and disc volume V. The calculated bulk thermistiror resistivity ρ [Ωm] and density d [g/cm^3] vs. sintering temperature T_{sint} is given in Figure 5.a and 5.b respectively. The resistivity vs. residual porosity is given in Figure 5.c.

The wet printed NTC layer was around 55 μm thick (measured by optical microscope), the dried layer thickness was around 25 μm (dried at 150 °C/30 min) and after sintering at 850 °C /10 min the thickness was around 11.3 μm (measured by Planer 100, surface profiler). SEM imaging revealed that the average grain size was around 0.3 to 0.5 μm (Figure 6).

The measured sheet resistivity using the Du Pont resistor test geometry was 1.38 MΩ/square. The spacing between test electrodes was 25 mm and electrode effect on the thermistor layer (PdAg electrode diffusion into the edges of thermistor) lowered the sheet resistivity by around 10 to 20 %. In the sandwich thick film thermistor construction the spacing between bottom and top electrodes was around 30 μm. The NTC thermistor layer was three times printed and sintered sequentially. The electrode effect on the surface lowered the resistance of the sandwich resistor by around 0.1 kΩ. After that, the five sandwiches were connected in series in zig-zag direction and repacked to form novel construction called thick film segmented thermistor with reduced dimensions (see Figure 7). All the layers of the segmented thermistor (electrodes and NTC layer) were printed, dried and sintered at 850 °C/10 min sequentially. The resistance of segmented thermistor was increased in proportion with the number of segments (sandwiches) to R=500 to 700 Ω measured at room temperature, which is suitable for self-heating thermistor applications.

The NTC thermistor behavior vs. temperature was measured in the climatic test chamber Heraeus-Wötsch VK I 08/450 in the range from -20 to +120 °C; the results given in Figure 8.

The NTC curve of the thick film thermistor was used for calculating exponential factor B in the range from 10 to 30 °C using Steinhart-Hart equation [17] in the form such as (1).

$$B = \left[\frac{(T_1 \cdot T_2)}{T_2 - T_1}\right] \cdot \ln\left[\frac{R_1}{R_2}\right] \quad \ldots\ldots (1)$$

where R_1 and R_2 are thermistor resistances measured in the climatic test chamber at temperatures T_1=283.16 K (10°C) and T_2=300.16 K (30°C). Using the values for resistances

R_1 and R_2 for temperatures T_1 and T_2 (see NTC curve in Figure 9) the exponential factor value was obtained such as B=3356 K.

The realized thermistor powder $Cu_{0.2}Ni_{0.5}Zn_{1.0}Mn_{1.3}O_4$, thick film paste and thick film segmented thermistors with reduced dimensions were optimized for self-heating thermistor applications. The custom requirement was to achieve the nominal resistance of around 0.5 kΩ, to allow self-heating current of around 50 mA at 12 Vdc voltage supply and power dissipation of around 1/2 W to flowing fluids.

The modified nickel manganite composition, mechanical treatment of initial metal oxide powders, calcination and powder milling for a prolonged time were performed to lower thermistor bulk resistivity. The mechanical treatment of the initial powders mixture was performed to enable homogeneous distribution of substituents before calcination and the formation of complex spinel. The partial substitution of Ni^{2+} and Mn^{3+} ions with $Cu^{(1+, 2+)}$ and Zn^{2+} ions in the spinel structure from octahedral to tetrahedral site contribute to a slight decrease in energy gap Eg and generation of polarized electrons which improve the conductivity of the thermistor as a semiconductor.

The nanostructure / microstructure development during the sintering process (Figure 2 and 3) prove that nano-particles were agglomerated and finally were re-crystallized to micron sized grains. The bulk resistance ρ of the pressed and sintered discs decreased from 30 to12 Ωm when T_{sint} was increased from 850 to 1250 °C. Also, a bulk density was increased to around 5,35 g/cm^3 at 1250 °C. The relative residual porosity p [%] was calculated using "monocrystal density" of around 5.5 g/cm^3 estimated from the behavior of density in Figure 5.b. The minimum of residual porosity p of 4,75% (obtained at 1250 °C) is related to bulk resistance ρ of around 12 Ωm (Figure 5.c). For example, the disc thermistor of 9 mm diameter and 2mm height showed a decrease of the nominal resistance from around 70 kΩ to around 20 kΩ. This step was promising, but insufficient to fulfil the custom requirements.

The next step was the forming a thick film paste to reduce the thermistor high resistance due to disc thickness. The thick film sintering temperature profile was 850°C/10 min and the Du Pont test resistor (2.5 x 2.5 mm) exhibited high sheet resistivity of 1.38 MΩ/square as a consequence of sintering at much lower temperature and forming so called "dendrite" thick film structure with numerous open cavities (Figure 6). This structure is a consequence of a low initial

density of NTC layer (screen printing), burning of the cellulose as an initial organic vehicle of the powder and a low sintering profile in a hybrid conveyor furnace (850°C/10 min).

The desired lowering of thickness between two electrodes was realized latter by printing sandwich thermistor geometry. The novel thick film thermistor geometry was generated with two rows of PdAg electrodes and NTC layer in the middle (Figure 7).

This construction was applied to optimize the resistance to desired values which fit the custom requirements. The obtained NTC curve for this construction (Figure 8) has moderate slope, and calculated thermistor exponential factor B= 3356 K is suitable for self-heating thermistor applications. The dimensions were reduced by two times, the reduction of voltage supply 10 times, self-heating current increased up to 2,5 times, and power saving around 2 times compared to the initial nickel manganite thermistor (table I). These optimizations were based on the novel thermistor paste and novel thick film thermistor construction.

4. Conclusion

Thick film thermistor pastes are rarely commercial products, more often products that are custom designed to specific requirements. The process from thermistor powder synthesis and paste forming and characterization usually lasts more than a few months and needs engagement of laboratory and researchers specialized in thick films.

- The synthesis and characterization of thermistor paste based on $Cu_{0.2}Ni_{0.5}Zn_{1.0}Mn_{1.3}O_4$ as a novel grade show that modification of $NiMn_2O_4$ by substitution of Mn and Ni with Cu and Zn results in lowering thermistor resistance by several times. However, the thick film thermistor resistance depends on the type of thermistor construction and electrode effect due to PdAg diffusion into thermistor layer.

- In this work both problems were solved by using the novel custom designed thermistor paste and the novel construction named thick film segmented thermistors with reduced dimensions. The authors tested these advances in thick film thermistors on two sensors such

as heat loss flowmeter for water and heat loss anemometer and now continue the work on their improvement [21-22].

Acknowledgement

This study was supported by the Ministry of Education, Science and Technological Development of the Republic of Serbia, and these results are parts of the Grant No. 451-03-68/2020-14/200132 with University of Kragujevac - Faculty of Technical Sciences Čačak.

5. References

1. E.D. Macklean, *Thermistors*, Electrochem. Pub., Glasgow, 1979, pp. 5-22.
2. F. J. Hyde, *Thermistors*, First Edition, Published by ILIFFE, 1971, pp. 2-15.
3. P. R. N. Childs, J. R. Greenwood, C. A. Long, Review of temperature measurement, *Review Scientific Instrumentation*, Vol. 71 (8), pp. 2959-2965, 2000.
4. T. D. Mc Gee, *Principles and Methods of Temperature Measurement*, John Wiley,1988, pp. 2-21.
5. S. Filipović, N. Obradović, Lj. Andjelković, D. Olćan, J. Petrović, M. Mirković, V. Pavlović, D. Jeremić, B. Vlahović, A. Đorđević, Multiferroic $BaTiO_3$/ϵ-Fe_2O_3 composite obtained by in situ reaction, *Science of Sintering*, Vol.53(1), 2021, pp.1-8.
6. Vesna Paunović, Zoran Prijić, Vojislav V. Mitić, Effect of donor and acceptor dopants on the microstructure and dielectric properties of barium titanate based ceramics, *Science of Sintering*, Vol.54 (1), 2022, pp. 81-91.
7. R.C. Buchanan, *Ceramic Materials for Electronics: Processing, Properties and Applications* (Electrical Engineering & Electronics), Marcel Dekker Inc; Enlarged 2nd edition, 1986, pp. 125-162.
8 T.G. Nanov, S.P. Yordanov, *Ceramic Sensors: Technology and Applications*, Chapter 5 Thermistors, CRC Press, 1996, pp. 193-203.
9 R. Metz, Electrical properties of N.T.C. thermistors made of manganite ceramics of general spinel structure: $Mn_{3-x-x'}M_xN_{x'}O_4$ ($0 \leqslant x + x' \leqslant 1$; M and N being Ni, Co or Cu). Aging phenomenon study, *Journal of Materials Science*, Vol. 35, pp. 4705–4711, 2000.
10. C. Ma, Y. Liu, Y. Lu, H. Gao, H. Qian, J. Ding, Preparation and characterization of $Ni_{0.6}Mn_{2.4}O_4$ NTC ceramics by solid-state coordination reaction, *J Materials Science: Materials in Electronics*, Vol. 24 (12), pp. 5183–5188, 2013.
11 H. Zhang, A. Chang, C. Peng, Preparation and characterization of Fe^{3+}-doped $Ni_{0.9}Co_{0.8}Mn_{1.3-x}Fe_xO_4$ ($0 < x < 0.7$) negative temperature coefficient ceramic materials, *Microelectronic Engineering*, Vol. 88 (9) pp. 2934–2940, 2011.
12 E. S. Na, U. G. Paik, S. C. Choi, The effect of a sintered microstructure on the electrical properties of a Mn-Co-Ni-O thermistor, *Journal of Ceramic Processing Research*, Vol. 2 (1), pp. 31- 34, 2001

13. M. Vakiv, O. Shpotyuk, O. Mrooz, I. Hadzaman, Controlled thermistor effect in the system $Cu_xNi_{1-x-y}Co_{2y}Mn_{2-y}O_4$, *Journal of the European Ceramic Society*, Vol. 21, pp. 1783–1785, 2001.
14. O. Shpotyuk, A. Kovalskiy, O. Mrooz, L. Shpotyuk, V. Pechnyo, S. Volkov, Technological modification of spinel-based $Cu_xNi_{1-x-y}Co_{2y}Mn_{2-y}O_4$ ceramics, *Journal of the European Ceramic Society*, Vol. 21 (11-12), pp. 2067–2070, 2001.
15. D. Fang, C. G. Lee, B. H. Koo, Preparation of Ultra-Fine FeNiMnO4 Powders and Ceramics by a Solid-State Coordination Reaction, *Metals and Materials International*, Vol.13 (2), pp.165-170, 2007.
16. K. Park, Microstructure and electrical properties of $Ni_{1.0}Mn_{2-x}Zr_xO_4$ ($0 \le x \le 1.0$) negative temperature coefficient thermistors, *Materials Science and Engineering* B, Vol. 104 (1-2), pp. 9-14, 2003.
17. K. Park, D.Y. Bang, Electrical properties of NiMn-Co(Fe) oxide thick film NTC thermistors, *Journal of Materials Science: Materials in Electronics*, Vol. 14, pp. 81-87, 2003.
18. S. Jagtap, S. Rane, S. Gosavi, D. Amalnerkar, Preparation, characterization and electrical properties of spinel-type environment friendly thick film NTC thermistors, *Journal of the European Ceramic Society*, Vol. 28 (13), pp. 2501-2507, 2008.
19. K.V.Harypria, S.V.Sharon, A.K.Malini, Tailoring the Properties of Ni-Mn Based NTC Thermistors by Cu and Li Addition, *Physica Scripta*, Vol.96 (12), 2021, pp.125728.
20. L. Dongcai, H. Cangbao, W. Ranran, X. Haiyan, Z. Fengjun, The Effects of Sn Doping $MnNiFeO_4$ NTC Ceramic: Preparation, Microstructure and Electrical Properties, *Materials* (MDPI), Vol.15, 2022, pp. 4274-4286.
21. S. O. Aleksić, N. S. Mitrović, Z. Nikolić, M. D. Luković, N. N. Obradović, S. G. Luković, Three-axis' heat loss anemometer comprising thick-film segmented thermistors, *IEEE Sensors Journal*, Vol. 19 (20), 2019, 10228-10235.
22. S. O. Aleksić, N. S. Mitrović, M. D. Luković, S. G. Luković, N. T. Nikolić, Heat Loss Flowmeter for Water Based on Thick Film Thermistors in Power Save Regime, *IEEE Sensors Journal*, Vol. 21(1), 2021, pp. 199-206.

Садржај - Прах за наменски термистор састава $Cu_{0.2}Ni_{0.5}Zn_{1.0}Mn_{1.3}O_4$ је добијен користећи одређену смешу металних оксида и реакцију у чврстом стању на 1000 °C/4h у атмосфери ваздуха. Добијени термисторски прах је млевен до субмикронског праха у кугличном планетерном млину и ахатном млину у продуженом периоду времена. Затим је добијени прах карактерисан помоћу XRD и SEM технике. После тога термисторски прах је пресован у испреске облика малог диска и синтерован на 1150 °C/2h. Синтеровани узорци су такође карактерисани помоћу XRD и SEM. Основна електрична својства као што је номинална отпорност R и термисторски експоненцијални фактор B су мерени у клима комори. После тога припремљена је дебелослојна паста користећи исти прах, органски носилац прахова и прах везивног стакла. Паста је штампана на алумина подлогама, сушена 150 °C / 30 min и синтерована у ваздуху на 850 °C / 10 min у хибридној конвејерској пећи. Планарне електроде су штампањем PdAg дебелослојне пасте нанете на синтеровани NTC термисторски слој. Електрична своства синтерованог дебелослојног термистора су такође мерена у клима комори. Добијени резултати су коришћени за развој нових термистора који се самозагревају.

Кључне речи: NTC дебелослојни термистор; модификовани никл манганитни прах.

Figures:

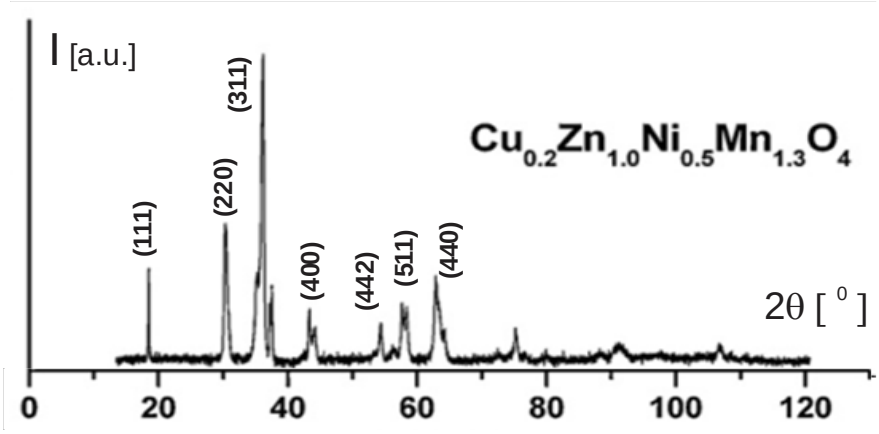

Fig. 1. XR diffractogram of novel submicron thermistor powder based on modified nickel-manganite (after final milling to submicron particle size).

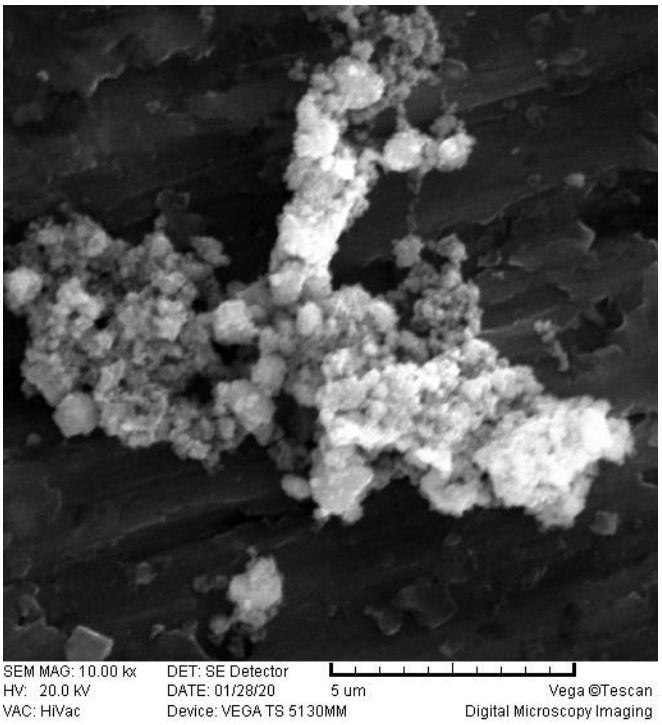

Fig.2. SEM image of the structure of agglomerated $Cu_{0.2}Ni_{0.5}Zn_{1.0}Mn_{1.3}O_4$ submicron thermistor powder.

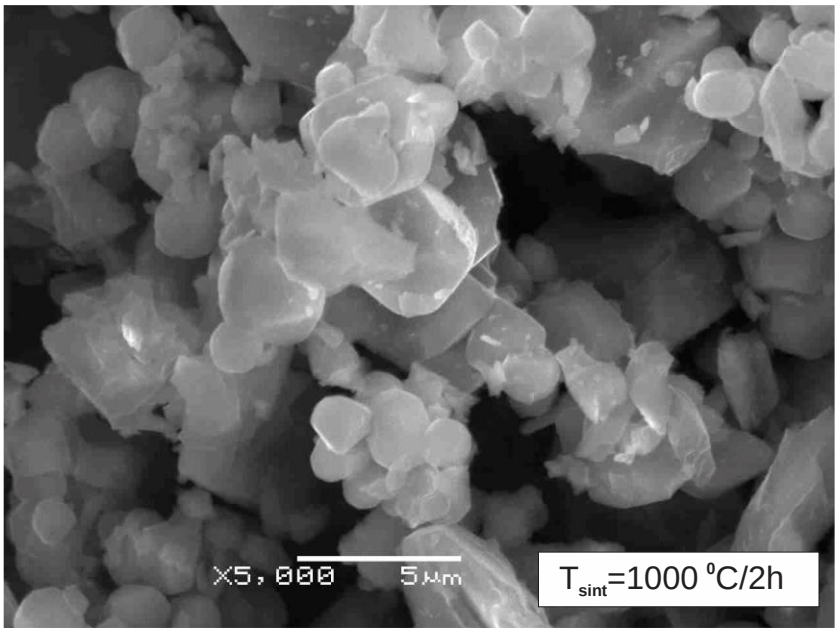

Fig.3. SEM of pressed and sintered $Cu_{0.2}Ni_{0.5}Zn_{1.0}Mn_{1.3}O_4$ at 1000° C/2h- the fracture of the disc sample.

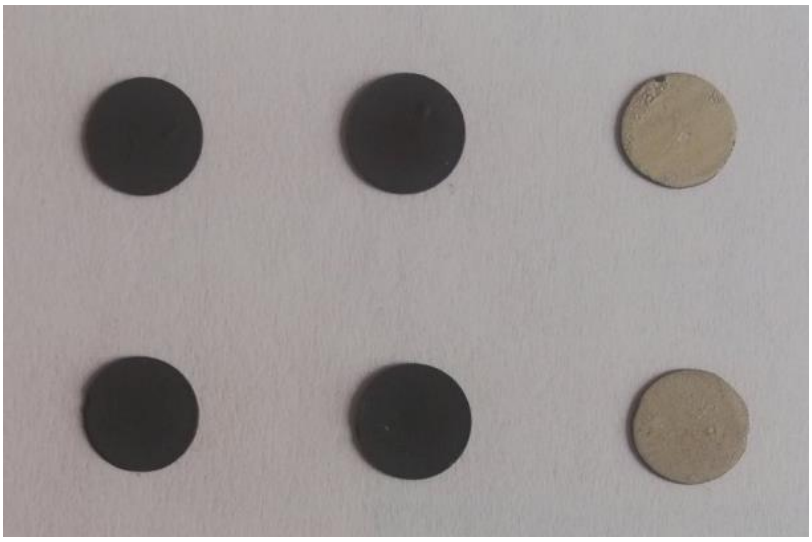

Fig.4. The disc thermistors $Cu_{0.2}Ni_{0.5}Zn_{1.0}Mn_{1.3}O_4$ with silver electrodes.

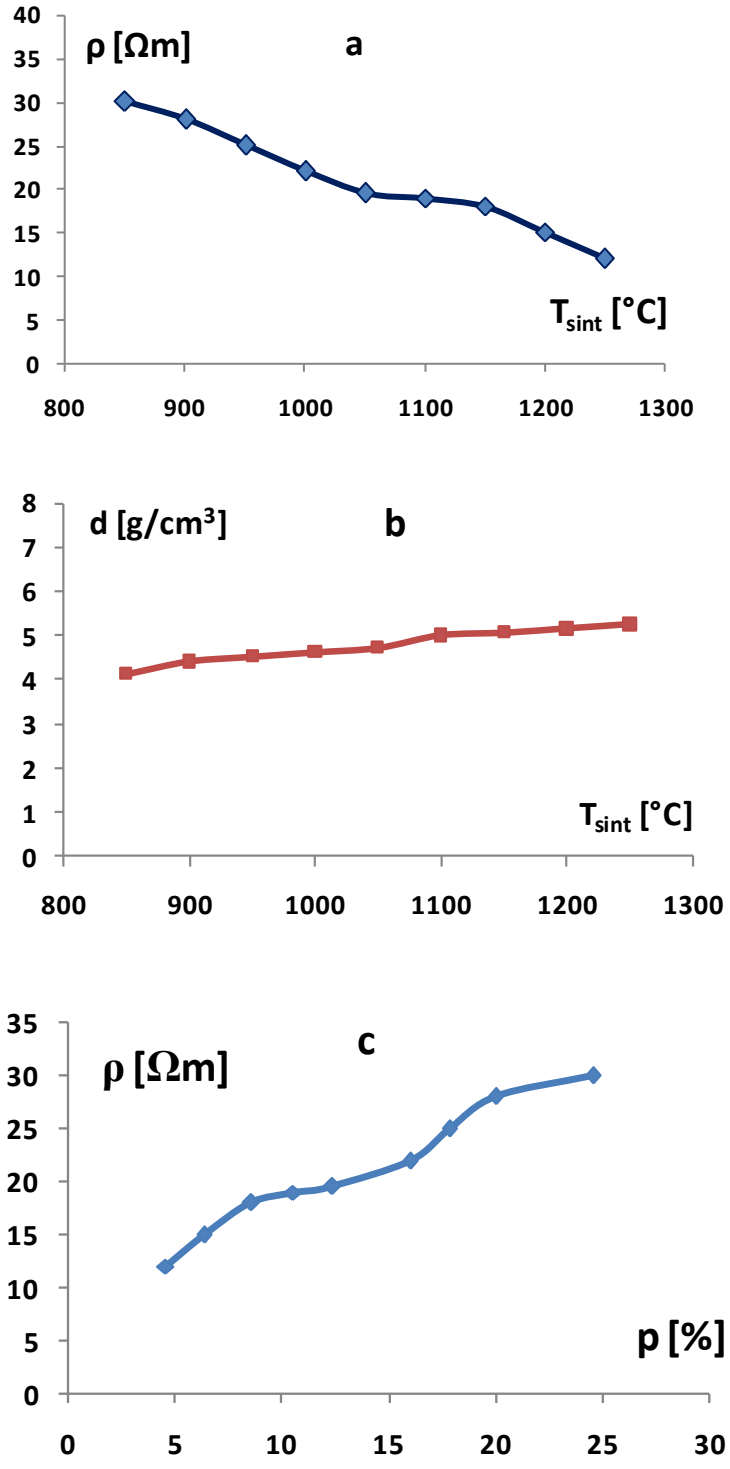

Fig.5. The resistivity ρ (curve a) and density d (curve b) of $Cu_{0.2}Ni_{0.5}Zn_{1.0}Mn_{1.3}O_4$ sintered disc thermistors vs. sintering temperature T_{sint} and resistivity ρ vs. relative residual porosity p (curve c).

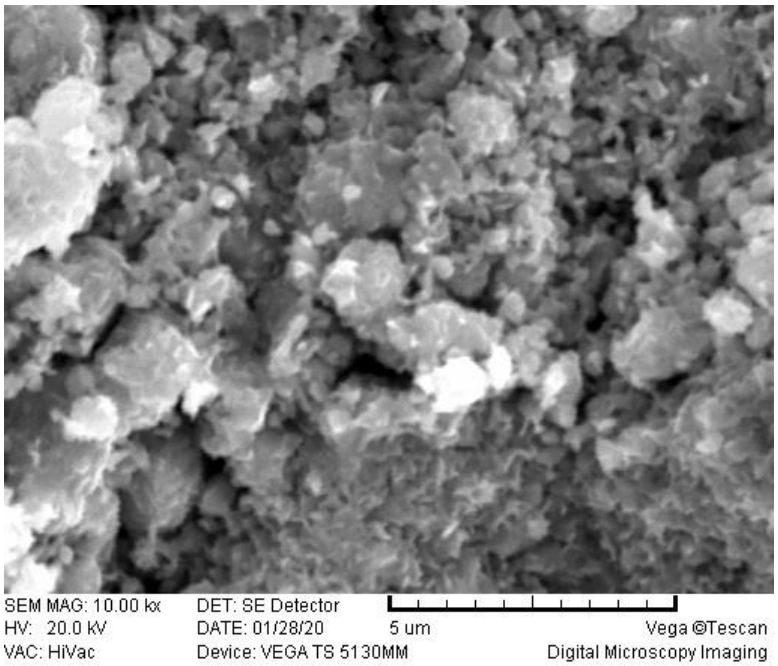

Fig.6. The thick film structure of $Cu_{0.2}Ni_{0.5}Zn_{1.0}Mn_{1.3}O_4$ sintered at 850°C/10 min in the conveyor furnace (top view).

Fig.7. Thick film thermistor with reduced dimensions: a-bottom electrodes (gray), b- NTC layer (black) and c- top view of the full construction. Actual size of alumina substrate (white): 25 · 6.35 · 0.5 mm.

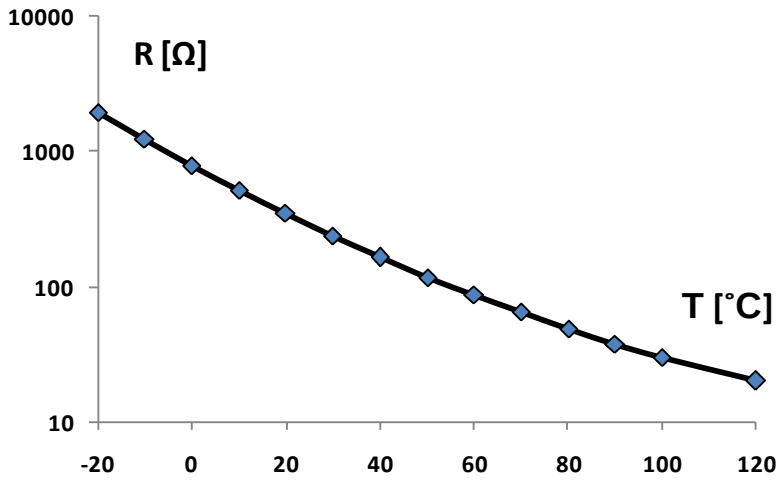

Fig. 8. NTC curve of sintered $Cu_{0.2}Ni_{0.5}Zn_{1.0}Mn_{1.3}O_4$ thick film segmented thermistor with reduced dimensions.

Table I: Comparison of thick films thermistor pastes

Material grade	$NiMn_2O_4$	$Cu_{0.2}Ni_{0.5}Zn_{1.0}Mn_{1.3}O_4$
B [K] -thermistor exponential factor	3860	3356
Segmented thermistor dimensions [mm]	50,8 x 12,7 x 0,5	25,4 x 12,7 x 0,5
Thermistor layer thickness [µm]	36,5	36,2
R_0 [Ω] - thermistor resistance at 20°C	6018,5	590,3
max dissipation power [W]	1	0,5
max self-heating current [mA]	25	65